THE JOURNAL OF COMPARATIVE NEUROLOGY 246:527-543 (1986)

Cell Generation, Death, and Retinal Growth in the Development of the Hamster Retinal Ganglion Cell Layer

D.R. SENGELAUB, R.P. DOLAN, AND B.L. FINLAY
Department of Psychology, Cornell University, Ithaca, New York 14853

ABSTRACT

During the early postnatal period in the hamster, the retinal ganglion cell layer grows, establishes its central connections, and undergoes substantial cell loss. In this study, we describe the development of the retinal ganglion cell layer with particular attention to the creation of local specializations in cell density. Changes in the number and spatial distribution of cells identified by a single ^3H thymidine injection were examined through the period of maximal cell loss (postnatal days 4–10) and at adulthood.

The cells of the retinal ganglion cell layer are generated from embryonic day 10 to postnatal day 3. Overall, cell number in the ganglion cell layer increases by approximately 108,000 cells (223%) from postnatal day 1 to 5, because of continued migration of cells generated prenatally. Cell number decreases from postnatal day 5 to 10 (25%), coincident with the presence of degenerating cells. Cell type is correlated with day of generation: the largest cells, all having retinal ganglion cell morphology, are generated on embryonic days 10 and 11; intermediate-sized cells predominantly of ganglion cell morphology on embryonic day 12; and smaller cells of displaced amacrine or glial cell morphology thereafter.

At adulthood, the hamster retina shows a streaklike elevation of cell density through central retina. However, at the time of maximal cell number (postnatal day 5), cell density is uniform across the retina. During the period of cell degeneration, cells are lost in greater relative numbers from the retinal periphery. This cell loss occurs principally from the first-generated cells (embryonic days 10 and 11), as shown by both changes in the distribution of labeled cells and by the spatial pattern of labeled degenerating cells. From postnatal day 10 to adulthood, relative cell density continues to decline in the periphery of the retina, thus suggesting that differential growth completes the production of the adult cell density distribution.

Key words: visual streak, retinogenesis, cell degeneration

The distribution of cells in the retinal ganglion cell layer of most vertebrates is not uniform, showing areas of elevated cell density such as the visual streak in rabbits and the area centralis in cats and primates (Stone, '83). Although these distributions and the cell types that compose them have been well described in adult animals, how these specializations arise during development is as yet incompletely understood. Four mechanisms that could singly or together produce these specializations have been suggested: greater cell generation in areas of later high cell density, greater death of cells in areas of eventual lower density, greater growth or expansion of areas of later low cell density, and migration of neurons toward areas of greater densities (Stone et al., '82; Sengelaub and Finlay, '82; Mastronarde et al., '84; Beazley and Dunlop, '83).

In several species with typical mammalian central retinal specializations, the initial distribution of cells in the retinal ganglion cell layer is either homogeneous or considerably flatter than the adult distribution (ferret, Henderson et al., '85; cat, Stone et al., '82; quokka, Beazley and Dunlop, '83; human, Provis et al., '85), showing that differential adult

Accepted December 16, 1985.

densities are not produced by differential cell generation alone. Differential retinal growth has been implicated in the development of the area centralis in the cat (Mastronarde et al., '84), but it may not be sufficient alone to account for the entire cell density disparity (Stone et al., '82). In the hamster, the incidence of degenerating cells in the periphery of the retinal ganglion cell layer is higher than in the center during the first postnatal week (Sengelaub and Finlay, '82), suggesting differential cell death could account at least in part for the higher cell density of hamster central retina at adulthood.

Tritiated thymidine autoradiography has been used to study the development of the rodent retina, and the time of origin and subsequent migration and differentiation of several cell types has been established. Cells of the retinal ganglion cell layer are generated first, and cells of the outer layers are generated progressively later (Sidman, '61; Braekevelt and Hollenberg, '70; Morest, '70; Carter-Dawson and LaVail, '79; Hinds and Hinds, '83). There is considerable overlap in generation times for all cell types, and while there is general agreement that substantial numbers of cells are generated in all locations on each generation day, investigators differ on the degree to which spatial patterns can be distinguished. For all retinal layers, the general pattern observed is that initially cells are generated in both central and peripheral areas, while at later times cells are generated only at the retinal periphery (Sidman, '61; Carter-Dawson and LaVail, '79).

In this study, we examined the contribution of three factors, differential generation, growth, and death, to the production of the central specialization of the hamster retinal ganglion cell layer. We first describe the changing spatial distribution and density of cells in the ganglion cell layer of the hamster over the first 10 postnatal days. During this period central retinal connections are established, and cellular degeneration is maximal (Frost et al., '79; Wikler et al., '85; Sengelaub and Finlay, '82). To trace the fate of these cells through development to adulthood we used thymidine autoradiography. To examine the contribution of differential cell generation, we assessed the number and the initial spatial distribution of cells labeled on each day of retinal ganglion cell layer generation. To examine the contribution of cell death, we investigated changes in the number and spatial distribution of these cells, as well as the spatial pattern of labeled degenerating cells over the period of maximal cell degeneration. Finally, changes in the spatial distribution of labeled cells after the major period of cell death are used to infer processes that operate in later postnatal development to complete the production of the differential cell density in the hamster retinal ganglion cell layer.

METHODS

Retinae from a total of 111 hamsters (*Mesocricetus auratus*) were used (27 for the descriptive study and 84 for the autoradiographic studies).

Descriptive study

Three animals for each of postnatal days (P) 1, 2, 3, 4, 5, 6, 7, 8, and 10 were examined (postnatal day 1 = day of birth). Only animals delivered in the normal 15.5–16-day gestation period were used in order to match postconceptional ages.

Our methods for the preparation of retinal cross sections and the recognition and counting of normal and degenerating cells have been described in a previous paper (Sengelaub and Finlay, '82). Briefly, pups were overdosed with urethane and perfused intracardially with a 4% formalin/45% alcohol solution at standardized times to match postconceptional ages as closely as possible. Eyes were left in the snout to retain proper orientation, dehydrated, embedded in polyester wax, and sectioned horizontally at 10 μm. One retina from each animal was selected and five equally spaced sections through the extent of the ganglion cell layer were examined at 500×. This procedure was selected because it results in a total area of retina sampled ($\bar{x}$ = 3.3% ±0.2 SEM) that is comparable to that typically employed for retinal whole mounts. Because of the relative uniformity of the hamster's retinal cell density, this standardized sampling procedure appeared to capture the extant variability in cell density at all ages we examined. The number and position of normal and degenerating cells within the ganglion cell layer of each section were recorded, and cell numbers were corrected for frequency of encounter by cell size and section thickness by the method of Abercrombie ('46). Because of the minimal amount of cytoplasm and changing nuclear morphology of cells, it is not possible with Nissl-stained material alone reliably to categorize the various classes of cells in the ganglion cell layer during this period of development (Fig. 4, left; see also Perry and Walker, '80b). All cells, excluding vascular elements, were counted for this reason. With autoradiographic methods (see below), however, the identity of labeled cell groups can be confirmed by their morphological characteristics at adulthood. Degenerating cells were recognized by the standard criteria of nuclear pycnosis and clear cytoplasm (Chu-Wang and Oppenheim, '78; Cunningham et al., '81; Sengelaub and Finlay, '82; Young, '84). The incidence of these cells, expressed as a fraction of normal cells, has been shown to reliably predict changes in adult neuron number in the retina (Rager and Rager, '78; Sengelaub and Finlay, '81; Sengelaub et al., '83; Perry et al., '83; Wikler et al., '85; Raabe et al., '85).

The estimated total number of cells per retinal ganglion cell layer was calculated by dividing the cell total of five sections by the fraction of the total retinal ganglion cell layer the five sections composed.

Autoradiographic procedures

For this part of the study 84 hamster pups from 16 litters provided the retinae used. Following mating at a standard time, pregnant females were injected once intraperitoneally wth methyl-tritiated thymidine (5 μCi/g body weight, specific activity 20 Ci/mM, New England Nuclear) on one of embryonic days (E) 9–14. The 24 hours following mating was designated as E0 and by this count pups were deliverd on E15 (E15 = P1). For postnatal injections, pups were injected individually on one of days P1–6. All injections were done at a standardized time to minimize any possible diurnal variations in uptake.

We have previously established the time course of cellular degeneration in the retinal ganglion cell layer (P1–P10, peaking days P5–P6; Sengelaub and Finlay, '82). For this experiment, we first surveyed the entire period of retinogenesis (E9–P3) for the number and distribution of labeled cells and labeled degenerating cells on P4, prior to maximal cell degeneration, and days P5 and P6, the period of maximal cell degeneration. Using the results of this survey, we then focused on changes in the spatial distribution of cells generated on the first 3 days of retinogenesis, when cells of

TABLE 1. ^{3}H Thymidine Injection Day and Day of Animal Death for Autoradiography Studies

Injection day	Examination days P4	P5	P6
A. Thymidine injection and examination schedule for survey, n/cell			
E9	2	2	2
E10	2	2	2
E11	2	2	2
E12	2	2	2
E13	2	2	2
E14	2	2	2
E15(P1)	2	2	2
P2	2	2	2
P3	2	2	2
	Examination days P6[1]	P10	P30
B. Selective examination of major generation days, n/cell			
E10	4	4	3
E11	4	2	3
E12	4	3	4
E14	3	2	2
			Total n = 84

[1]n includes animals from Survey, Table 1A.

retinal ganglion cell morphology are generated (E10, E11, and E12), and 1 later generation day (E14) when cells of primarily displaced amacrine and glial morphology are generated. For convenience we will refer to the group of cells labeled by a single thymidine injection as a "cohort." We assessed changes in the distribution of the E10, E11, E12, and E14 cohorts on P6 (the peak of cell number in the retina, and a partial replication of the first series), P10 (the end of the major period of cell death), and P30 (when the distribution is indistinguishable from the adult). Table 1 shows the distribution of animals by injection day and day of animal death.

Autoradiographic processing

Preparation of retinal cross sections was identical to that used in the descriptive study except for the particular requirements of the autoradiographic procedure. For each developmental series, all animals were littermates whenever possible to maximize comparability of injection. Cross sections were mounted on acid-cleaned slides, dipped in Kodak NTB-2 nuclear track emulsion, and stored in dessicated light-proof boxes at 4°C for 28–54 days. Test developments were done at regular intervals to insure comparability of exposure. Extent of labeling was kept low so as not to obscure nuclear detail critical for recognition of degenerating cells. Retinae from an injection series were processed as a group to minimize any possible variability in emulsion, exposure, and developing. Following exposure, slides were developed in D-19 and counterstained through the emulsion with cresylecht violet.

Because it was necessary that animals be littermates to minimize variability in gestational age and thymidine delivery, the number of animals in each developmental series is limited. Since appropriate caution must be used in interpreting the results from these small samples, we have looked for converging results and agreement between independent measures over the three studies to support observations made in any one.

The close postconceptional age in the P4–P6 series allowed their histological processing to be identical, and this series was used for assessment of changes in absolute numbers of labeled cells in each cohort during the period of maximal cell degeneration, as well as for the spatial distribution of labeled cells. For the P6/P10/P30 group only changes in the spatial distribution of labeled cells were assessed, and no estimation of the absolute amount of cells labeled was attempted.

Cell counting procedures

For the P4–P6 series, ten equally spaced sections through the retinal ganglion cell layer were selected. For animals examined at P4 or P6, five equally spaced sections were taken from these 10 and drawn and counted at 750×, noting the locations, numbers, and silver grain densities of all cells (both normal and degenerating) in the ganglion cell layer. The alternate five sections were examined only for the location and number of labeled and unlabeled degenerating cells. For animals examined at P5, only counts of labeled degenerating cells were made.

For the P6/P10/P30 group, six equally spaced sections were chosen and counted at 750× as above with a camera lucida/graphics tablet and computer system for labeled and other cells. At P30, measurement of soma diameter and qualitative description of labeled cells was made.

For the P4–P6 series, in order to consider a cell labeled the number of silver grains over its nucleus had to exceed a criterion of five times the background grain density of the section (Sidman, '70). Background grain counts were determined for each section by calculating the density of silver grains over adjacent cell-free areas. No significant differences in background density across injection day were found, nor did the density of the labeling of the most heavily labeled cell vary across groups. In all cases, this criterion allowed only the inclusion of cells with grain counts greater than half the grain count of the most heavily labeled cells. For the P6/P10/P30 series, cells were considered labeled if their grain count exceeded half the grain count of the most heavily labeled cells.

Numbers of normal and degenerating cells were corrected by the method of Abercrombie ('46), and estimated total numbers of cells in the ganglion cell layer (labeled and overall) for each retina were calculated as described below. The incidence of cell degeneration was calculated by using the ratio of degenerating cells to normal cells with separate ratios determined for total degenerating cells (per 1,000 live cells) and by cohort (labeled degenerating cells per 1,000 labeled live cells).

Representational techniques

For graphical representation of the changing number of cells in the ganglion cell layer in standard retinal sectors over development, each of the horizontal retinal sections for each eye were divided into six equal segments, and the cell number in the segment calculated. For comparability of cell number per segment across each retina and across days, cell number in each segment was normalized in three ways. First, since oblique cuts through the retina will increase the sample of the retinal ganglion cell layer artificially, cell counts in each segment were adjusted for obliquity. For the early postnatal retinae, the width of the outer neuroblastic layer (the presumptive receptor/bipolar layers) was measured at the midpoint of each of the six segments of each section. The width of the outer neuroblastic layer is consistent, thinner nasally than temporally, but with little or no systematic variation on the superior to

inferior axis. Thus, any variation in thickness from superior to inferior was assumed to be the result of an oblique cut through the retina. After averaging the outer neuroblastic layer widths within a section, the cell counts for that section were adjusted by the ratio of that section's mean outer neuroblastic layer width to the thinnest mean outer neuroblastic layer width for each eye. For the P10 and P30 retinae, which approximate spheres more closely, the correction for obliquity was derived from the Pythagorean theorem, the inner and outer radius of the ganglion cell layer, and the superior-inferior section level (height), with this formula:

$$\text{correction factor} = \frac{\sqrt{(r_2^2 - h^2)} - \sqrt{(r_1^2 - h^2)}}{r_2 - r_1}$$

where r_1 = inner circumferential length of the retinal ganglion cell layer (rgcl)/π, r_2 = outer circumferential length rgcl/π, and h = section level on the superior to inferior diameter of the retina where h = 0 at the midpoint of that diameter.

Secondly, since sections differed in length as a result of the level of the section through the retina, cell numbers per segment were divided by the fraction each was of the longest segment per retina. Third, to be able to compare cell number across days, each corrected segment number was divided by the percent area counted for that retina. The resultant cell number per standard retinal sector, normalized for obliquity, segment length, and percent area counted is represented as a height in the cell density plots.

Since absolute labeled cell number was not computed for the P6/P10/P30 series, only the obliquity and length corrections were made, and the density in each sector was expressed as a percent of the summed sector densities for the entire retina. For example, if cell density in the retina were uniform and there were 36 retinal sectors, each sector would have a percent value of 100/36 = 2.78. Alternatively, if all of the labeled cells were found uniformly in the 18 central sectors with none in the periphery, each central sector would have a percent density value of 5.56, and the peripheral sectors percent density would equal 0. To determine changes in spatial distribution of cells over days, corresponding sector values were subtracted to give relative density changes (Figs. 10, 11).

Because autoradiography requires sectioning and cannot be done with flat-mounted materials, the traditional representation of absolute densities on actual or schematic retinal whole mounts with isodensity contours was not possible. However, the necessity to section the material offers several advantages as well. For example, flat-mounting often introduces distortions in cell density at cut edges and retinal margins. Sectioned material requires that the retina be reconstructed, but fewer differential stretch and shrinkage artifacts are introduced, a factor of central importance for this study.

This data analysis (cell density per retinal sector) is designed to capture changes in relative, but not absolute, cell density. It should be emphasized that it is not necessary nor do we make the assumption that the sectors represent the same physical part of the retinal ganglion cell layer over development, which would assume uniform retinal growth. However, the changing numerical composition of all sectors can be used to infer growth or local cell addition or loss.

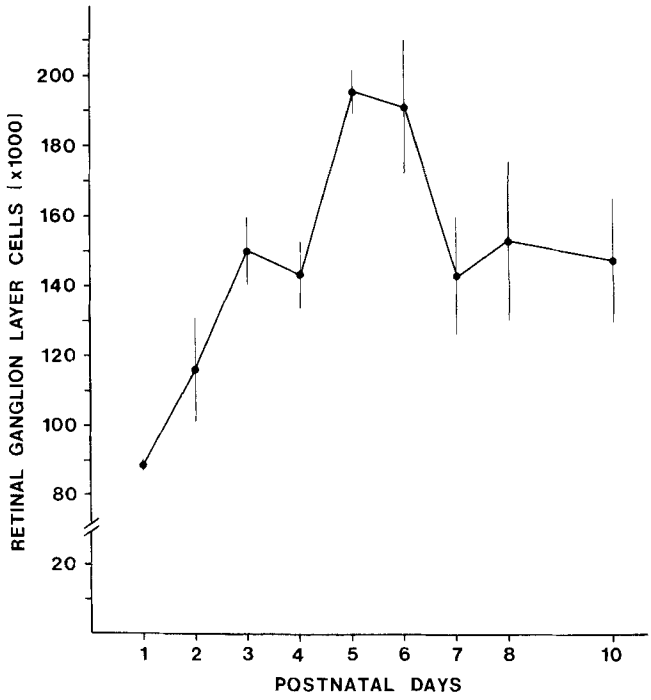

Fig. 1. Estimate of total cells in the ganglion cell layer over the first 10 postnatal days. Points represent averaged values (N = 3 per day) ± SEM.

RESULTS

Cell number and distribution

Figure 1 shows the changing number of cells in the hamster retinal ganglion cell layer over the first 10 postnatal days. There is a significant increase in average cell number from P1 to P5 of 108,000 (223%; t = 15.95, df = 4, P < .01; P1 $\bar{x}$ = 87,800 ± 2,200; P5 $\bar{x}$ = 195,600 ± 6,600) after which there is an average loss of 48,000 cells (25%), which is also significant (t = 2.56, df = 4, P < .05; P10 $\bar{x}$ = 147,600 ± 17,600). This cell number includes retinal ganglion cells, "displaced" amacrine cells, and glia, whose relative contribution to total cell number changes over this period (as discussed below in the autoradiographic results). Cellular degeneration in the ganglion cell layer (Fig. 3) can be seen throughout the periods of both net addition and subtraction (Sengelaub and Finlay, '82). Since the magnitude of total cell subtraction unconfounded by cell addition during the first 10 postnatal days is not known, the absolute cell loss cannot be determined from these data. The loss of 25% of the cell population between P5 and P10 underestimates the actual loss because of continued cell migration into the ganglion cell layer between these days (Fig. 5, discussed below).

Figure 2 shows the changing distribution of cells in the retinal ganglion cell layer across the retina for postnatal days 1 and 2 (n = 6), 5 and 6 (n = 6), and 10 (n = 3). Retinal area has been equalized in this figure for ease of visual comparison; the retina in fact grows substantially during this period, with the cross-sectional length (through the optic disc) increasing from an average of 1.91 mm (± 0.02 SEM) at P1 to an average of 4.94 mm (± 0.32 SEM) at P10. For each age, the temporal to nasal pattern of cell densities

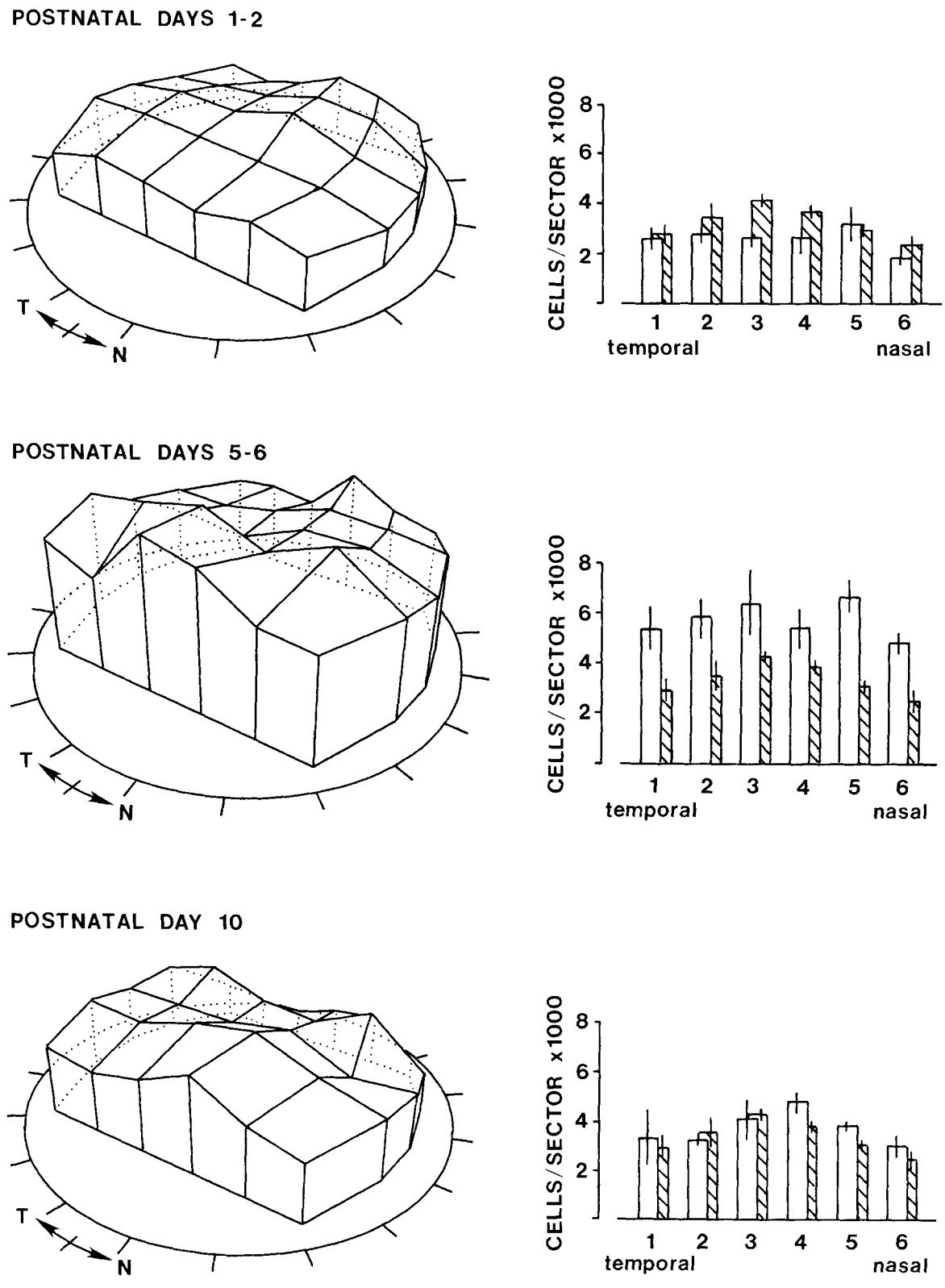

Fig. 2. Averaged cells per sector in the ganglion cell layer over the first 10 postnatal days (N = 6, postnatal days 1–2, 5–6; N = 3, postnatal day 10). Retinal diameters have been normalized to allow direct density comparisons. For each age, averaged cell number ± SEM in each of the six temporal to nasal sectors through the densest part of the ganglion cell layer (open bars) have also been plotted against the sector densities for the equivalent adult section (hatched bars) to aid in interpretation (T, temporal; N, nasal).

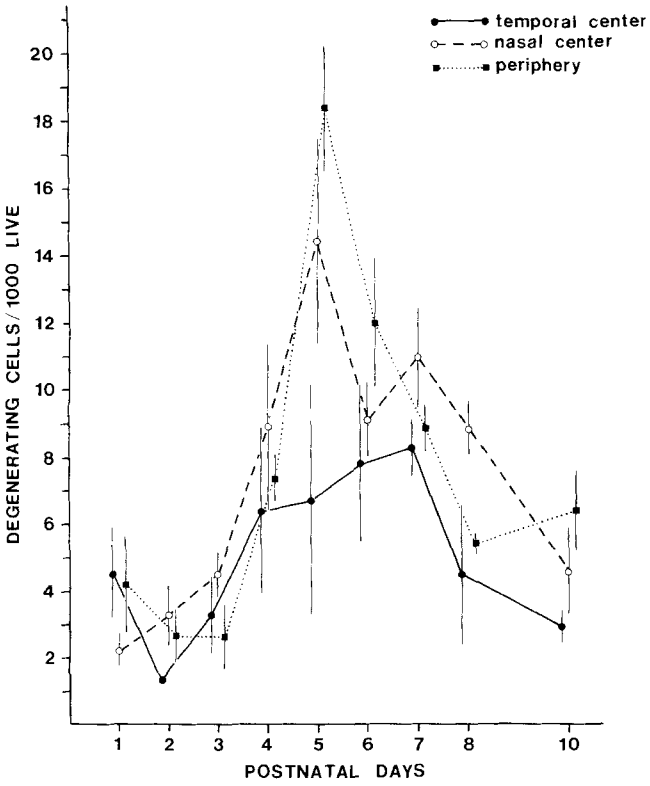

Fig. 3. Ratio of degenerating cells to normal cells in the ganglion cell layer over the first 10 postnatal days for the three retinal subareas: temporal center (solid lines); nasal center (dashed lines); and peripheral retina (dotted lines). Points represent averaged values (N = 3 per day) ± SEM.

taken from a horizontal section through central retina is compared to the relevant adult section (data from Sengelaub et al., '83). The histograms on the right of Figure 2 illustrate the relative variability in cell density per sector as well as directly compare those densities with their corresponding adult levels. On days P1 and 2, the distribution of cells in the retinal ganglion cell layer shows little differential elevation, and is flat compared to the adult distribution. On days P5 and 6, cell density is elevated and irregular in the ganglion cell layer. By P10, a center to periphery difference has emerged, and the distribution of cells in the central retina begins to resemble the adult distribution.

A formal analysis of the pattern of production of the P10 densities was done by correlating the sector densities of the initial distribution (P1–2), sector density changes during the period of net cell addition (P4–5 minus P1–2), and sector density changes during the period of net cell subtraction (P4–5 minus P10), each separately to the appropriate matched sector densities of the P10 distribution. The correlation of the P1–2 distribution with the P10 distribution is $r = .38$ and the regression equation ($y = 1{,}314 + 0.682x$) is significant [$F(1,28) = 4.91$, $P < .05$]. Given the large numbers of cells still to be added to the ganglion cell layer, this correlation probably reflects the spatial distribution of the earliest-generated cells (see E10, Fig. 6). The correlation of sector cell addition over P1 to P5 (P4–5 minus P1–2) with the P10 distribution is not significant [$r = .179$, $y = 2{,}624 + 0.214x$; $F(1,28) = 0.92$, $P > .25$]. The correlation of the difference distribution of P4–5 minus P10 with the P10 distribution is $r = -0.61$, $y = 3{,}812 - 0.592x$. This equation is highly significant [$F(1,28) = 16.72$, $P < .0005$]. These analyses indicate that significant alterations in cell density occur between P5 and P10, and by P10 the distribution of cells has begun to approximate the adult pattern of differential cell density. This finding carries no import for mechanism: continued cell addition, cell death, or retinal growth each could potentially produce this change in differential density.

The pattern of cell degeneration

We had previously observed that the incidence of cell degeneration was higher in the retinal periphery than in the central 90° (Sengelaub and Finlay, '82). In this study, we have subdivided the retina into areas that more closely approximate the adult differences in cell density (Sengelaub et al., '83). Each retina was divided into the 30 retinal sectors described above and then grouped to form the area of highest adult ganglion cell density (the six central temporal sectors), the area of intermediate cell density (the six central nasal sectors), and the area of lowest cell density (the 18 peripheral sectors). After subdividing the 27 retinae, the respective incidences of cell degeneration were calculated, expressing the amount of degeneration as a ratio of degenerating cells to normal cells (Fig. 3). Cell degeneration ratios for retinal subareas were found to relate inversely to adult cell density on all days of substantial cell loss, and the differences between these ratios are highly statistically significant [$F(2,54) = 6.62$, $P < .005$]. In the following section, using data from thymidine autoradiography, we discuss the potential magnitude of the center/periphery disparity in cell density attributable to differential cell degeneration, as well as the cell types which contribute to this disparity.

Autoradiographic analysis of generation and degeneration patterns

Examples of labeled cells generated on E10, E12, and E14 as they appear on P6 and at adulthood are shown in Figure 4. The hamster retinal ganglion cell layer is generated from E10 through P3, although the number of labeled cells is quite small after P1 (Fig. 5). Injections on E9 produce only a few labeled cells in the ganglion cell layer on postnatal examination. Injections on E10–P1 produce large numbers of labeled cells, especially those injections made on E12 and E14. From P4 to P6 there is evidence of a progressive change in neuronal number in the retinal ganglion cell layer for the major cohorts. For cells labeled on E10–E12 (the cells with retinal ganglion cell morphology, see below and Figs. 4, 12), the numbers of labeled cells in the ganglion cell layer decrease an average of 19% from P4 to P6. However, cells generated on E13 or later (cells with displaced amacrine or glial morphology) show an average increase of 84% from P4 to P6. There is a significant interaction of ^3H injection day with postnatal day [$F(7,16) = 6.58$, $P < .01$]. For these early generated cohorts (E10, E11, and E12, the presumptive retinal ganglion cells) the number of labeled cells decreases from P4 to P6 but planned comparisons showed no statistically significant differences. Planned comparisons of numbers of labeled cells at E14 and E15 (the presumptive amacrine and glial cells) were both highly significant [F's $(1,16) > 24.18$, $P < .001$]. This cell addition

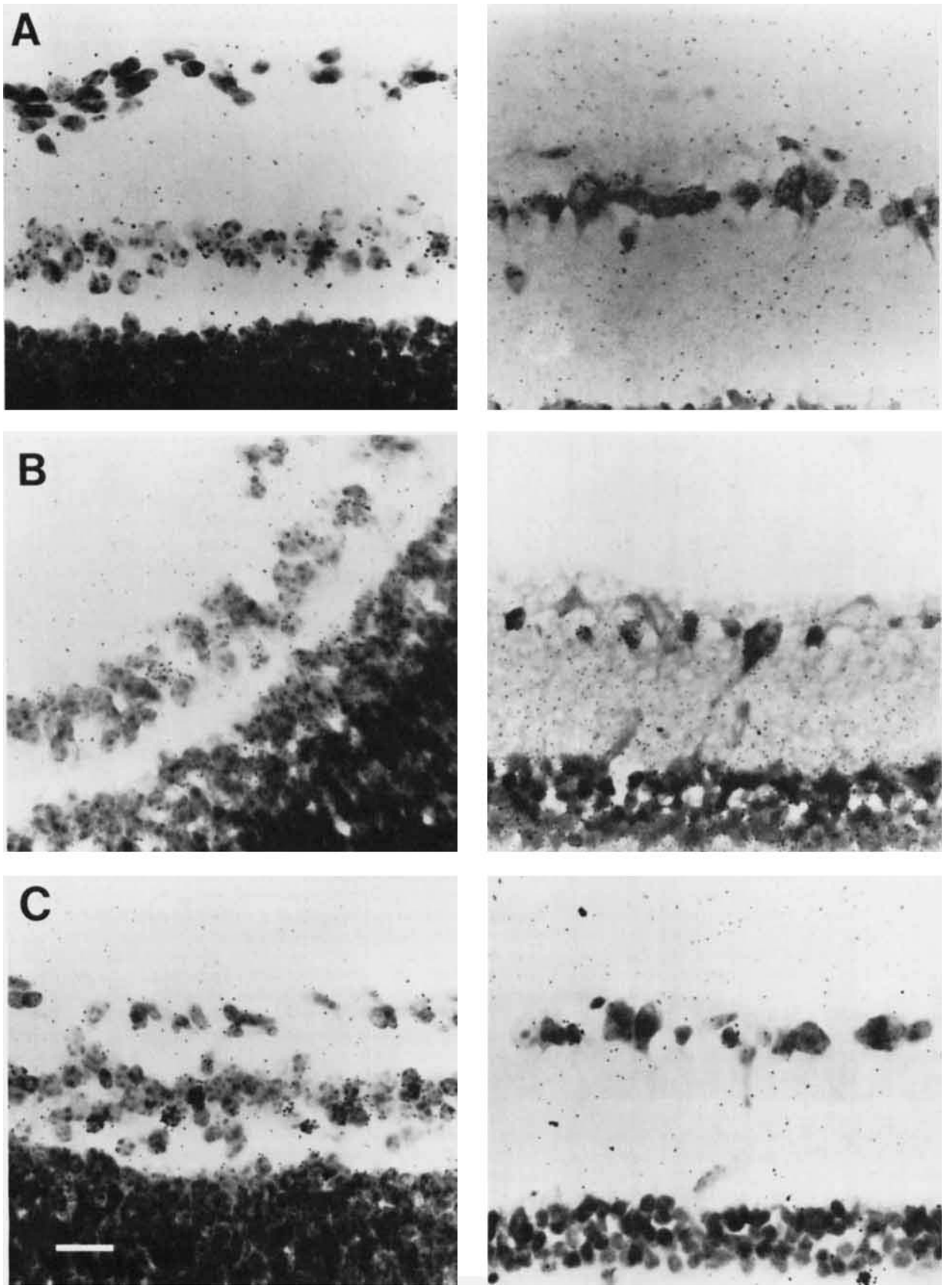

Fig. 4. Photomicrographs of the retinal ganglion cell layer at postnatal day 6 (left) and postnatal day 30 (right) after ^{3}H thymidine injections at embryonic days 10 (A), 12 (B), and 14 (C). Scale bar = 20 μm.

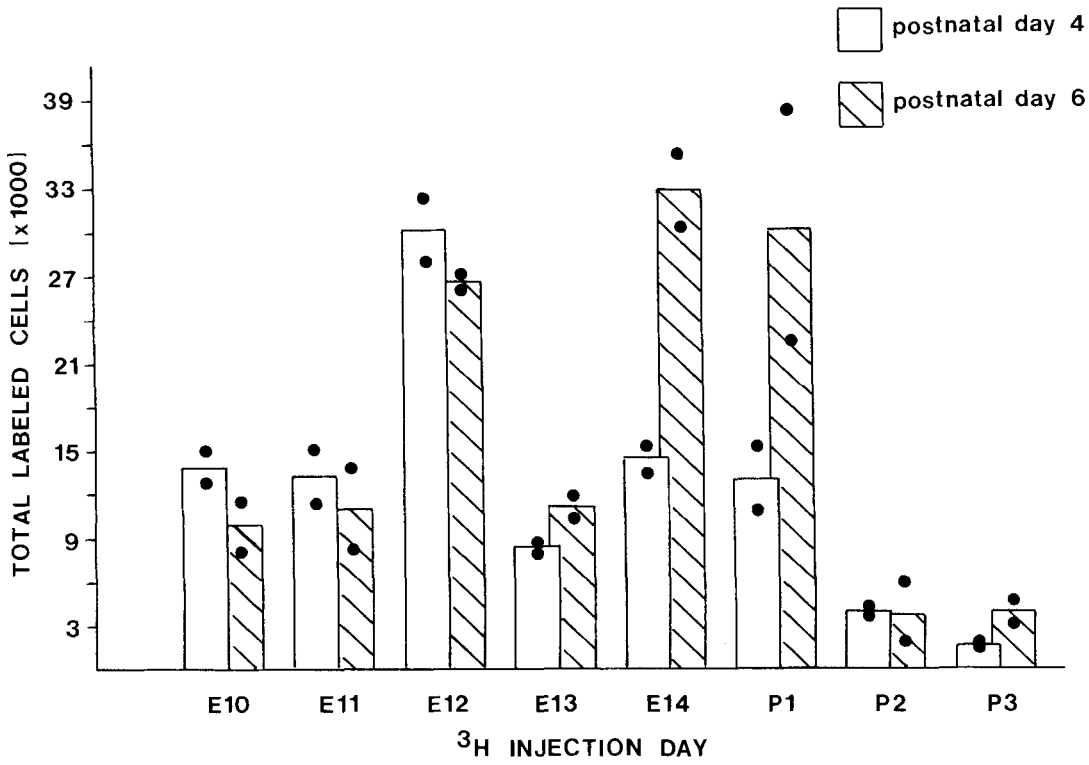

Fig. 5. Estimate of total labeled cells in the ganglion cell layer at postnatal days 4 (open bars) and 6 (hatched bars) after ^{3}H thymidine injections at embryonic day 10 through postnatal day 3. Points indicate estimates from individual animals (N = 2 per embryonic or postnatal day); bars represent averaged values.

can also be seen in total cell numbers (Fig. 1) after P4, and must thus be a prolonged migration of late-generated cells into the ganglion cell layer.

Spatial distribution of labeled cells by cohort

Figure 6 shows the spatial distribution of cell cohorts at their maximum in cell number in the ganglion cell layer (P4 for E10, E11, and E12 cohorts; P6 for E13, E14, and P2 cohorts). Each plot represents average sector cell densities (n = 2 per day) and in all cases the retinal diameters have been equated so that details of the distributions can be directly compared. Table 2 contains the individual animal data from which Figure 6 is drawn, and is provided for inspection of variability.

Cells destined for all retinal locations are generated on each generation day, but the spatial distribution of labeled cells varies with injection day and suggests a slight temporal to nasal and a larger center to periphery progression. For example, on E10, 32% more cells are labeled at the temporal margin of the retina than at the nasal margin, and 22% more centrally than peripherally. By E12, little center to periphery difference is present in cell generation (7% more peripherally) but a large shift in distribution of labeled cells nasally (46% greater than temporally) can be seen. Cells generated on E13 are located primarily at the retinal periphery, as are cells generated on E14 (26% more in the retinal periphery) and on E15 (52% more in the retinal periphery).

Maturational gradients in retinogenesis

Although cell generation patterns of the retinal ganglion cell layer show evidence of some spatial progression over days, there appears to be another, independent progression of maturation from superior-temporal to inferior-nasal retina that can be seen in a variety of indices of retinal development. If all cells in the ganglion cell layer are considered (Fig. 2), the cell loss in the superior-temporal retina precedes the cell loss of the inferior-nasal retina. The same pattern can be seen in changes in the labeled cohorts from P4 to P6. For example, cells labeled on E10 show an average decrement of 228 cells per sector in superior-temporal retina from P4 to P6, but a decrement of only 74 cells per sector in inferior-nasal retina. Similarly, for the E11 cohort there is an average decrement of 144 cells per sector in superior-temporal retina from P4 to P6, but only 80 cells per sector in inferior-nasal retina. Cell degeneration across all injection series shows a similar progression: the number of degenerating cells in superior-temporal retina is greater than that in inferior-nasal retina on P4, while on P6 there is a greater number of degenerating cells inferiorly. This same superior-temporal to inferior-nasal progression in rodent retinal development has been noted in several other

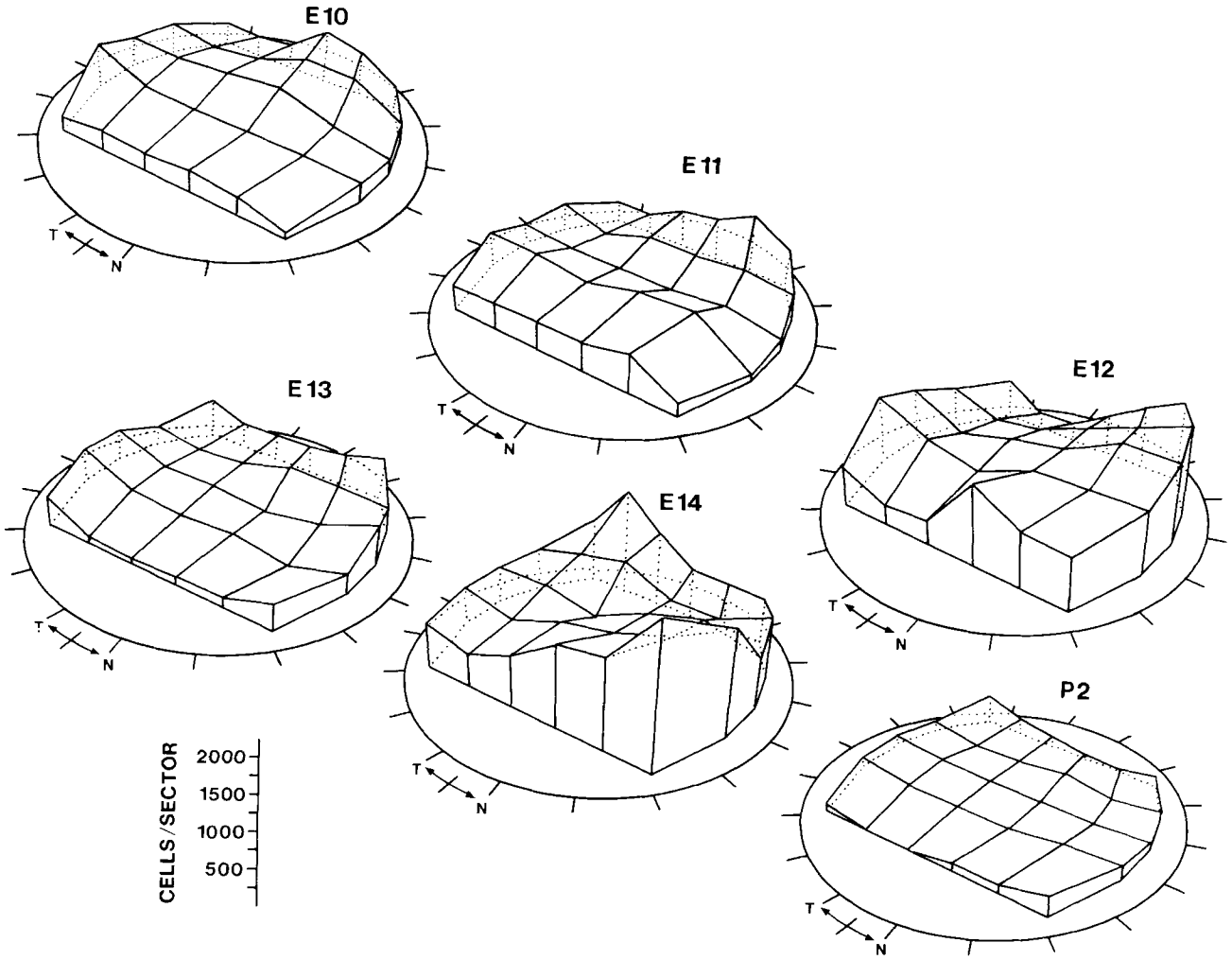

Fig. 6. Averaged labeled cells per sector in the ganglion cell layer at their postnatal maximum in cell number after ^{3}H thymidine injections at embryonic days 10–14 and postnatal day 2 (N = 2 per day). Retinal diameters have been normalized to allow direct density comparisons. Scale, identical in all cases, is shown at lower left (T, temporal; N, nasal).

contexts: in gross morphogenesis (Silver and Hughes, '73), initial axon outgrowth (Jhaveri and Schneider, '83), and initial contact with synaptic targets and cytochrome oxidase activity (Wikler et al., '85). It is curious that the spatial pattern of cell generation is apparently dissociable from other spatial gradients in maturation. Similar independence of generational and maturational gradients has been demonstrated in the superior colliculus (Cooper and Rakic, '83).

Cell loss by cohort

Labeled degenerating cells can be seen in the period of maximal cell death (Fig. 7). If the number of labeled degenerating cells summed over all cohorts is expressed as a fraction of the number of labeled normal cells summed over all cohorts for days P4 and P6, the ratio obtained is 15.3 labeled degenerating cells per 1,000 labeled normal cells, very close to cell death incidences obtained without considering labeling (Fig. 3), indicating that the potential to discern labeled thymidine in degenerating cells does not disappear faster than the degenerating debris itself.

The incidence of labeled degenerating cells appears markedly higher in the earliest-generated cohorts (E10 and E11) than in any other cohort on every postnatal day examined. The E10 and E11 cohorts, large ganglion cells, have a greater incidence of degenerating cells than the E12 and E13 cohorts ($t = 2.27$, $df = 10$, $P < .05$), which from adult morphology appear to be principally small ganglion cells (Figs. 4, 12). The incidence of degeneration in the E10 and E11 cohorts is also greater than that of cohorts generated on E14–P3 ($t = 2.63$, $df = 16$, $P < .01$), which appear to be principally displaced amacrine cells or glia.

Convergent evidence that supports the differences in the incidence of degenerating cells by time of generation can be found in the net decrement in labeled cell numbers from P4 to P6: 28% for E10, 17% for E11, and 12% for E12. If the

TABLE 2. Cells Per Sector Values for Individual Animals by Generation and Examination Day[1]

	(T)1	2	3	4	5	(N)6	(T)1	2	3	4	5	(N)6
E10/P4							E11/P4					
(S)1	247	374	607	819	487	384	50	128	241	240	502	474
	380	201	136	679	789	260	539	457	819	960	1188	630
2	327	365	337	592	805	231	136	69	276	233	190	136
	530	318	529	764	545	363	657	327	547	592	764	259
3	371	387	387	523	212	195	402	360	394	374	394	130
	479	468	615	664	478	242	184	96	70	80	245	221
4	548	355	513	368	399	266	606	606	546	808	781	114
	188	281	67	239	226	305	387	355	206	328	466	73
(I)5	243	244	236	330	359	139	101	176	194	136	236	67
	168	324	260	320	278	68	605	592	621	676	922	320
E12/P4							E13/P6					
(S)1	609	437	313	391	828	1062	626	323	546	538	676	631
	526	50	223	768	972	1235	469	370	199	240	124	576
2	452	290	223	350	569	741	219	187	42	483	418	225
	726	403	700	1147	1470	1788	327	150	422	386	426	557
3	541	169	278	458	711	1001	503	166	107	42	238	570
	982	600	927	1060	1583	1343	370	166	249	166	246	570
4	1029	343	272	436	677	986	457	219	95	106	35	238
	893	929	681	1180	1030	830	493	94	95	211	35	344
(I)5	442	221	306	1622	1261	725	346	161	118	207	238	235
	709	344	381	693	324	788	500	32	39	52	77	557
E14/P6							P2/P6					
(S)1	996	1593	1184	858	733	645	187	110	176	0	0	107
	837	1428	956	576	658	675	636	357	110	132	68	150
2	652	806	955	631	754	971	43	0	50	57	0	67
	545	724	856	566	451	841	242	42	47	213	47	218
3	520	594	428	798	989	773	39	0	0	49	0	62
	538	498	305	627	888	693	223	110	78	46	114	200
4	545	373	678	838	1131	1577	41	0	0	0	0	189
	526	335	609	752	1015	1414	233	35	35	39	312	235
(I)5	690	499	797	1300	1353	2165	46	0	0	62	45	35
	618	448	672	1054	1212	1941	171	0	0	172	209	584

[1]*Cells* per sector for individual animals in Figure 6 density plots. Densities from the two animals for each embryonic injection/postnatal examination day are listed in the six temporal (T) to nasal (N) sectors of the five superior (S) to inferior (I) retinal sections.

maturational gradient discussed previously is considered, and we examine only the superior-temporal half of the retina, where cell migration, axon outgrowth, and cell death are more advanced, the effect is amplified. In superior-temporal retina, 54% of the cells generated on E10, 36% of the cells generated on E11, but only 8% of the cells generated on E12 are lost. These calculations only reflect net changes in cell number, and it is possible that a continued migration of the later-generated cohorts into the ganglion cell layer between P4 and P6 could contribute to these results, although this seems unlikely in the case of the maturationally advanced superior-temporal retina.

Center/periphery differences in cell degeneration from P4 to P6

The incidence of overall cell degeneration is significantly higher in the retinal periphery than the retinal center from P4 to P10 (Fig. 3). Since some of the cohorts have a greater portion of their total cell number in the retinal periphery (Fig. 6; E12, E13, E14, and P2), an above-average cell loss in these cohorts could account for the increased cell loss in the periphery. For example, if the E14 cohort was preferentially and entirely lost, that alone would produce greater relative cell loss in the periphery overall. However, the opposite is true (Fig. 8); those cohorts that even slightly overrepresent the retinal center are the ones that show the greatest incidence of degeneration (E10 and E11).

To further describe the relationship between retinal position, time of generation, and cell death, degeneration indices for the central and peripheral retina over P4 and P6 were calculated for each cohort separately (n = 4 per generation day; Table 3). For each day of generation a ratio of central to peripheral degeneration was then computed (Fig. 9) such that ratios greater than 1 indicate higher degeneration incidences centrally, and less than 1 indicate higher degeneration incidences peripherally.

As can be seen in Figure 9, center/periphery cell degeneration ratios of the major generation-day cohorts are greater in the retinal periphery on E10, E11, and E13. Cells generated on E12 and E14 show an equivalent incidence of degeneration in central and peripheral retina. Thus, over the period of maximal cell degeneration, the first-generated cells (E10 and E11) show the largest amounts of degeneration, and that degeneration occurs principally in the peripherally located cells of those cohorts.

If time of cell generation and time of maximal loss were correlated, that is, late-generated cells also die later, it is possible that the P4–P6 window might only view the death patterns of the E10 and E11 cohorts. However, the day of

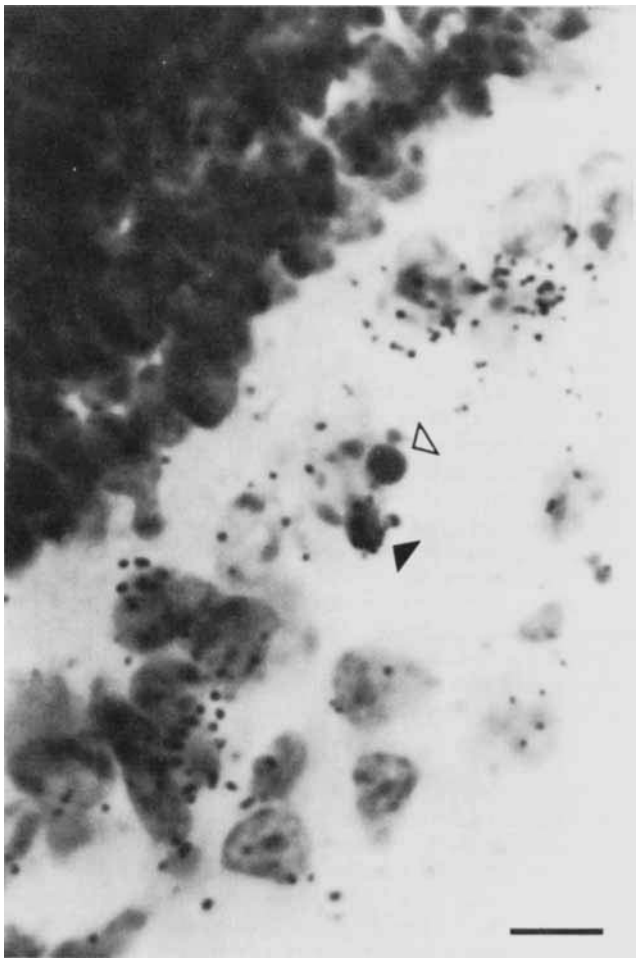

Fig. 7. Photomicrograph of the developing retinal ganglion cell layer after ^{3}H thymidine injection at embryonic day 10 showing a labeled (solid arrowhead) and an unlabeled (open arrowhead) degenerating cell. Scale bar = 10 μm.

TABLE 3. Center/Periphery Incidence of Labeled Degenerating Cells (Per 1,000 Labeled Live) for Each of the Major Generation Days[1]

	E10	E11	E12	E13	E14
Central retina					
Mean	22.35	32.74	10.94	13.04	13.27
SEM	9.84	19.62	3.61	4.66	6.56
Peripheral retina					
Mean	54.13	38.82	10.85	16.79	12.08
SEM	29.61	21.43	3.84	5.96	3.20

[1]Incidence of labeled degenerating cells per 1,000 labeled live cells in the center and periphery of the retina for each of the major generation days, averaged over P4 and P6 (n = 4 per generation day).

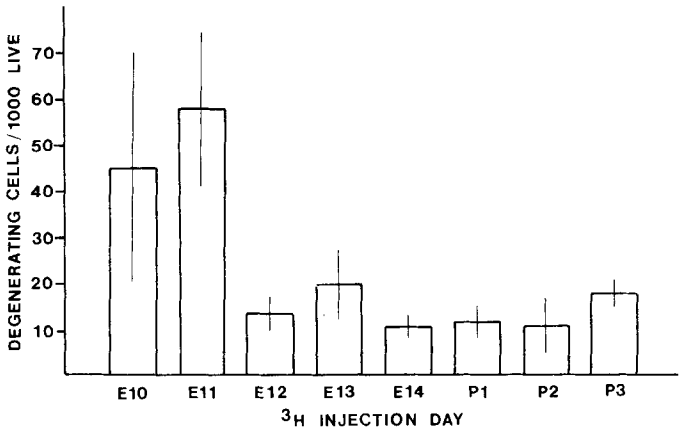

Fig. 8. Ratio of labeled degenerating cells to labeled normal cells in the ganglion cell layer during the period of maximal degeneration (postnatal days 5–6) after ^{3}H thymidine injections at embryonic day 10 through postnatal day 3. Bars represent averaged values (N = 4 per day) ± SEM.

maximal cell loss is P6 for every cohort from E10 to P1, with the exception of E13, whose loss is maximal on P5. Therefore, within this period there is no evidence that the day of maximal cell death and the day of generation are correlated.

Alterations in the spatial distribution of cells from P6 to P10

The difference from P6 to P10 in the relative percentage of the total distribution of cells in the retinal ganglion cell layer each retinal sector composes (for those areas that showed a decrease in relative density) is shown in Figure 10. Because this datum is expressed as a percentage, the sum of the changes in sector densities from P4 to P6 is equal to 1, and therefore computation of a central density constrains the peripheral density. However, for statistical analysis, a t test (which is sensitive to both direction and magnitude information) was considered appropriate because there is no a priori reason to assume that center and periphery density values were artifactually related.

The results are consistent with the pattern shown in the incidence of labeled degenerating cells: the E10 and E11 cohorts show a decrease in cell density in the periphery of the retina compared to the center, while the E12 and E14 cohorts show no obvious center-periphery differences. For E10, if the average sector density of the central 16 sectors is compared to the average sector density for the peripheral 20 sectors, the ratio is 1.08:1 on P6 (n = 4); by P10 (n = 4), the ratio has risen to 1.44:1, and a comparison of the density changes for the periphery compared to the center over this period shows a significant decrease in the periphery ($t = 1.72$, $df = 34$, $P < .05$). Similarly, the E11 center/periphery ratio rises from 1:1 to 1.43:1 from P6 (n = 4) to P10 (n = 2), and is also statistically significant ($t = 2.64$, $df = 34$, $P < .01$). By contrast, during this same time period, the E12 and E14 ratios remain unchanged (E12/P6 ratio = 0.60:1, n = 4; E12/P10 ratio = 0.53:1, n = 3; $t = 0.67$, $df = 34$, ns; E14/P6 ratio = 0.75:1, n = 3; E14/P10 ratio = 0.87:1, n = 2; $t = -0.52$, $df = 34$, ns). These results indicate that spatial distributions of labeled cells undergo different changes over the same time period. Thus, it is unlikely that any factor that would affect all cohorts similarly, such as retinal growth, could be the sole cause for development of the greater central cell density.

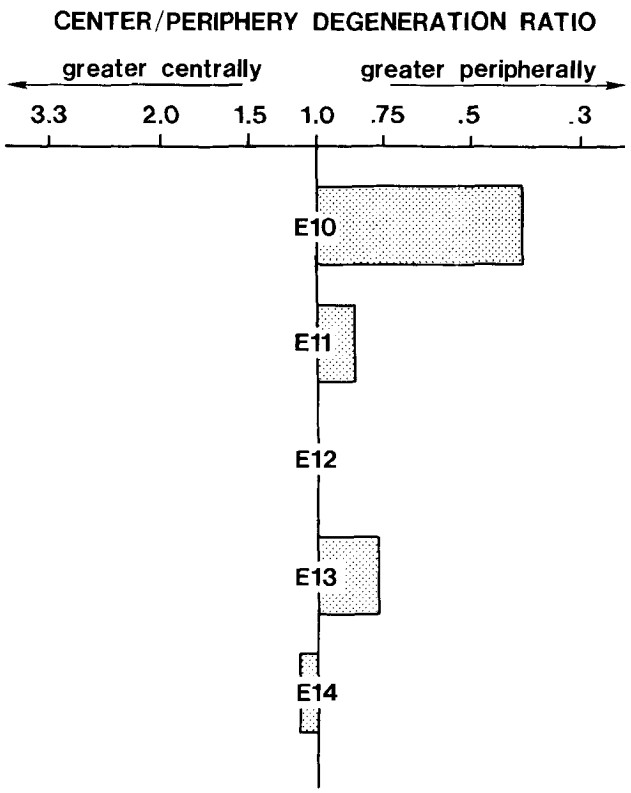

Fig. 9. Ratio of center/periphery degeneration incidence for each labeled cohort over the period of maximal degeneration after ^{3}H thymidine injections at embryonic days 10–14. Values greater than 1 indicate greater degeneration centrally; values less than 1 indicate greater degeneration peripherally (N = 4 per day).

Alterations in the spatial distribution of cells from P10 to P30

By P10, the incidence of degenerating cells in the retinal ganglion cell layer is approaching zero (Fig. 3), and the number of cells, but not their distribution, in the ganglion cell layer is very close to adult values (Fig. 1; Sengelaub et al ., '83; Fig. 2). By P30, however, the distribution of cells in the ganglion cell layer has reached its adult state. Alterations in relative cell density for each retinal sector for those areas that show density decreases are shown in Figure 11. All of the distributions appear to change in a similar manner, decreasing in relative density in the temporal and nasal periphery, which is reflected in their center/periphery density ratios at P30 (E10, 2.87:1, n = 3; E11, 1.35:1, n = 3; E12, 1.28:1, n = 4; E14, 1.70:1, n = 2). All of the density changes but E11 reach statistical significance (E10, $t = -3.17$, $df = 34$, $P < .01$; E11, $t = 0.29$, $df = 34$, ns; E12, $t = -4.02$, $df = 34$, $P < .01$; E14, $t = -3.33$, $df = 34$, $P < .01$). The fact that the distributions change similarly over the same period suggests that in the very late postnatal period, some mechanism common to all the distributions, like differential retinal growth, operates to produce the final cell distribution. Between P10 and P30 the retina continues to grow, increasing to an average cross-sectional length (through the optic disc) of 7.35 mm ± 0.72 SEM.

Correlation of cell diameter with day of generation

Although the identification of cell types in the retinal ganglion cell layer by using Nissl-stained material is somewhat problematic, we have used the classic criteria of soma shape and size, nuclear appearance, and Nissl inclusion to classify cell types by day of generation. Ganglion cells, characterized by their granulated-appearing nucleus with nucleolus, irregular soma shape, and abundant Nissl substance in their cytoplasm, compose the majority of the larger-sized cells at maturity (Chalupa and Thompson, '80; Perry and Walker, '80b; Perry et al., '83; Sengelaub et al., '83). Smaller cells, with darker, homogeneously staining nuclei, little cytoplasm, and few Nissl granules, are also present in the ganglion cell layer in large numbers, and these have been identified as displaced amacrine cells (Perry, '81; Perry et al., '83). Soma sizes at P30 associated with each day of generation are shown in Figure 12. The E10 and E11 cohorts typically have large soma diameters, and almost every labeled cell encountered has the nuclear appearance and cytoplasmic development associated with retinal ganglion cells with centrally projecting axons. The E12 cohort has smaller cell diameters, but for almost every cell encountered, the morphology of typical retinal ganglion cells. The cells generated on E14 also have small somas, and typically darkly staining nuclei with little cytoplasmic development, characteristic of displaced amacrine cells or glia in Nissl-stained material (Fig. 4).

DISCUSSION

Although each of the three studies described here is limited in terms of data or the conclusions that can be made, we have relied on the convergence of evidence across these studies in order to develop hypotheses about the basic mechanisms that underlie the development of the differential cell density in the ganglion cell layer of the hamster. Similarities between changes in overall cell number and the changes in the number of labeled cells both over time and spatially, or the relative incidence of degenerating cells, labeled degenerating cells, and observed declines in cell numbers are examples of such convergence. In the following discussion we attempt to bring together the converging lines of evidence as well as point out their limitations.

Magnitude and time course of cell addition and loss

The first 10 postnatal days in the hamster are a period of massive changes in cell number in the retinal ganglion cell layer. From P1 to P5, the number of cells in the ganglion cell layer more than doubles. As demonstrated by thymidine autoradiography, this cellular addition is due to the prolonged migration of cells generated prenatally, rather than to the *in situ* gliogenesis that is often sited as the cause of early postnatal cell number increases. Late migrating cells in the ganglion cell layer have been observed before (Sidman, '61), although the magnitude of the migration was not described. Retinal ganglion cells, displaced amacrine cells, and glia all appear to contribute to the postnatal addition, with the retinal ganglion cells the primary component in the early postnatal period, and displaced amacrine cells thereafter. In Golgi material, Morest ('70) has observed that axon outgrowth to the optic nerve can precede arrival of retinal ganglion cell somas into the retinal ganglion cell layer in early postnatal development. Perry et al. ('83) have also observed a substantial postnatal

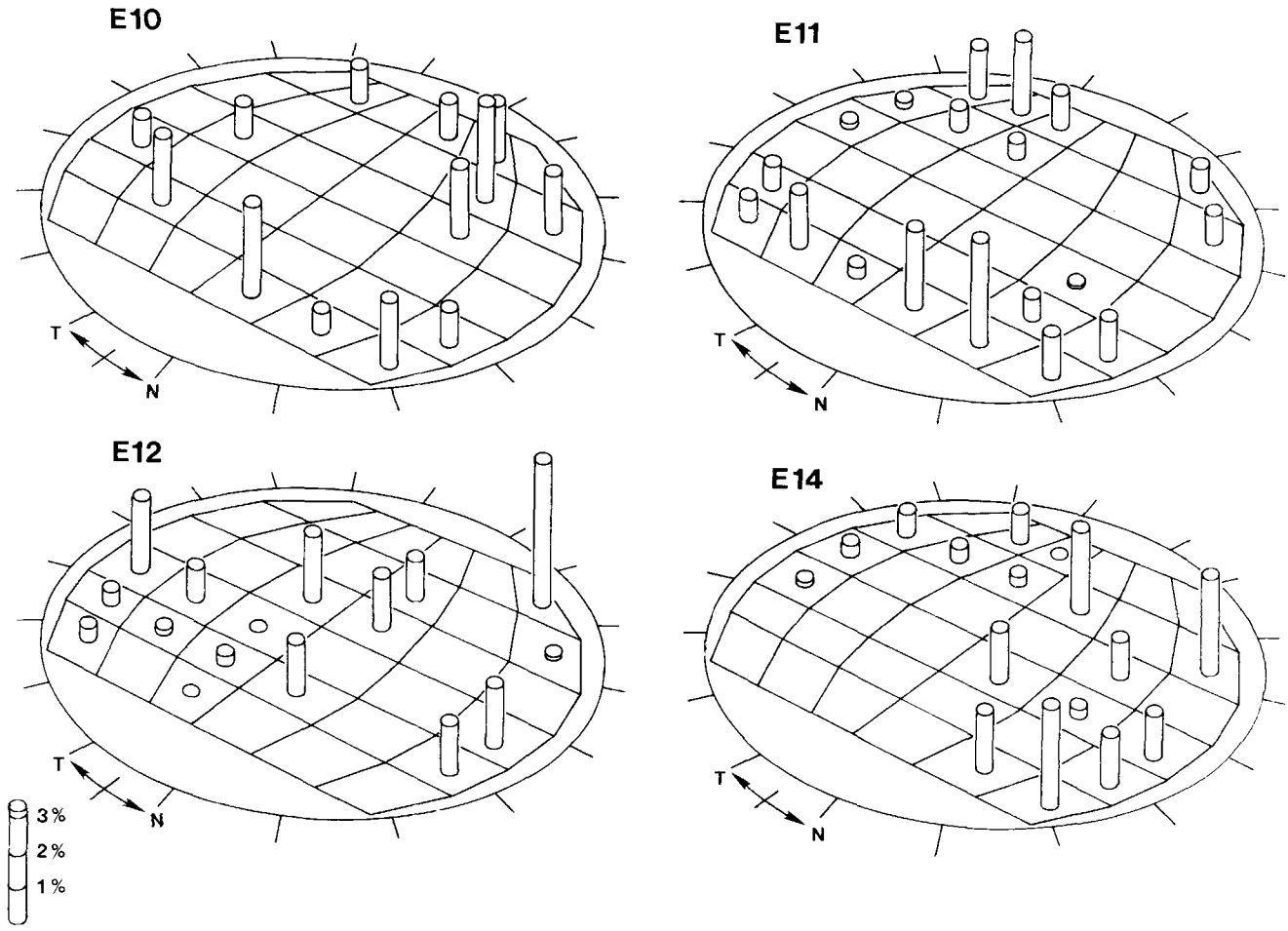

Fig. 10. Relative labeled cell density decrease per retinal sector in the ganglion cell layer from postnatal day 6 to postnatal day 10 after ^{3}H thymidine injections at embryonic days 10, 11, 12, or 14. Scale, identical in all cases, is shown at lower left. Each plot represents the differences in average relative sector density from postnatal day 6 (N = 3–4 per day) to postnatal day 10 (N = 2–4 per day) (T, temporal; N, nasal).

amacrine cell migration to the retinal ganglion cell layer in the rat.

Large decreases in cell number and optic nerve axon counts have been described for other mammals (Perry et al., '83; Potts et al., '82; Williams et al., '83; Rakic and Riley, '83; Beazley and Dunlop, '83). Using several estimation techniques to determine cell loss from the frequency of degenerating cells, we had previously calculated the magnitude of the cell loss to be approximately 50%, a figure comparable to that reported in the rat using counts of cells retrogradely labeled with HRP (Perry et al., '83). Our estimates of the total number of cells in the ganglion cell layer show a 25% cell loss that underestimates the actual loss because of continued cell migration into the ganglion cell layer. The autoradiography results support this magnitude estimate, and also show that the incidence of cell loss varies markedly by cohort.

Generational and maturational gradients in the retina

Center to periphery gradients in retinal neurogenesis in the rodent have been demonstrated previously (Sidman, '61; Carter-Dawson and LaVail, '79) and also in the cat (Walsh et al., '83). Prior to cell death and retinal growth, the spatial distribution of cells in the ganglion cell layer of the hamster indicates that the center-periphery gradient in cell generation is slight (Fig. 6). In fact, only on E10 are more cells produced centrally than peripherally, and on every other day the retinal periphery shows a slight (E11 and E12) or major (E13 to P2) advantage in neurogenesis.

By maturity, a center-to-periphery gradient in generation over embryonic days is apparent, but this gradient appears to develop from postgenerational events like cell death and differential retinal growth. For example, the E10 cohort is at its maximum in cell number in the ganglion cell layer at P6, and at this time the distribution of cells of this cohort have a center:periphery density ratio of 1.08:1. At maturity however, the center:periphery density ratio of this cohort has increased to 2.87:1. Thus, this finding suggests that the common assumption that the pattern of neurogenesis can be revealed by the examination of adult material is in error.

Alternative measures of maturation of the retina show a pattern quite distinct from the pattern of neurogenesis. A superior-temporal to inferior-nasal gradient can be seen in

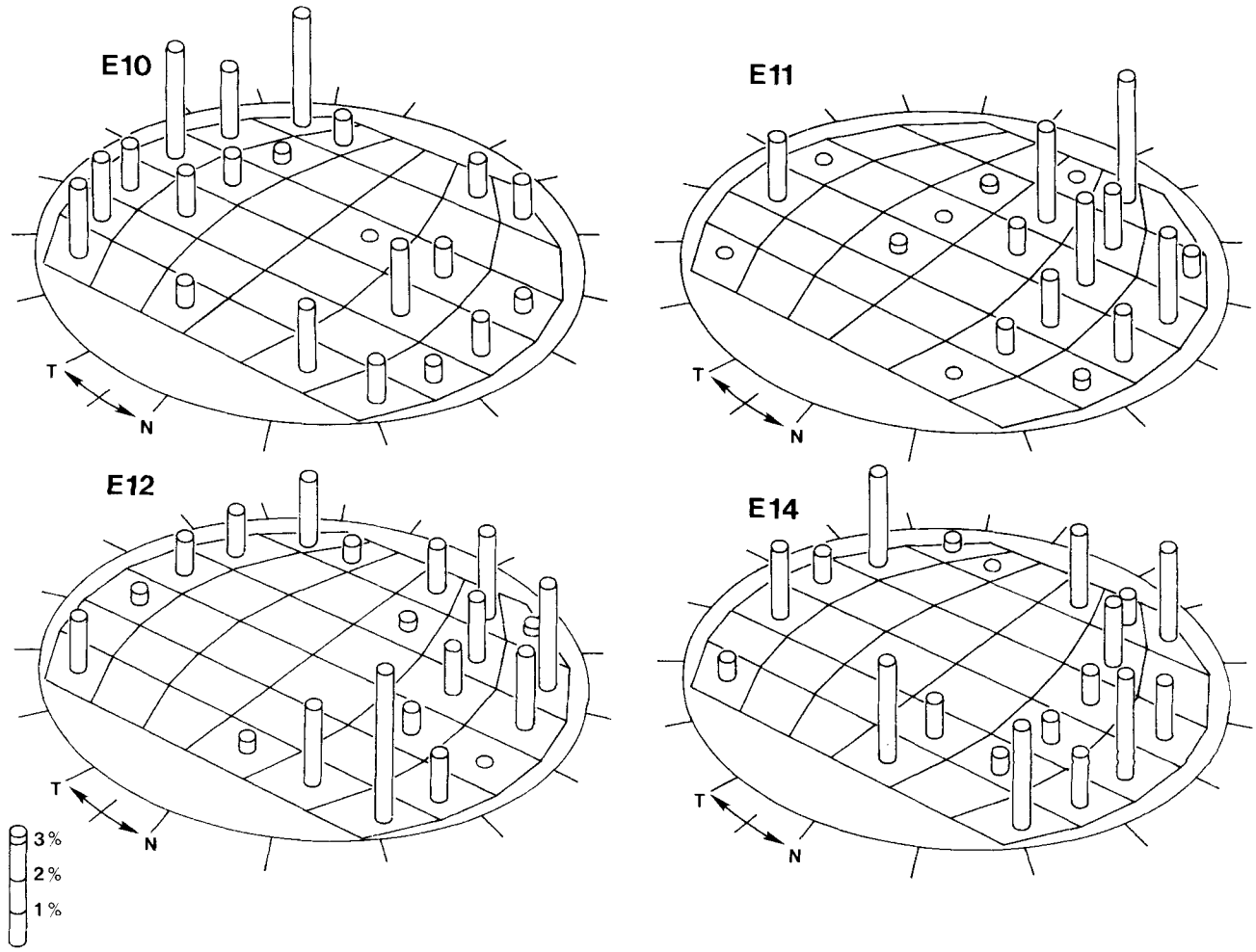

Fig. 11. Relative labeled cell density decrease per retinal sector in the ganglion cell layer from postnatal day 10 to postnatal day 30 after ^{3}H thymidine injections at embryonic days 10, 11, 12, or 14. Scale, identical in all cases, is shown at lower left. Each plot represents the differences in average relative sector density from postnatal day 10 (N = 2–4 per day) to postnatal day 30 (N = 2–4 per day) (T, temporal; N, nasal).

the original involutions producing the eyecup and stalk, as well as the attendant necroses (Silver and Hughes, '73); development of the intrinsic fiber layers (Rapaport and Stone, '82); the exit of the first optic axons from the retina (Jhaveri and Schneider, '83); the first contact of central visual targets and the development of cytochrome oxidase activity (Wikler et al., '85); and the progress of cell death across the retina (Cunningham et al., '81; this study). Interestingly, a similar pattern of differential maturation (which is retinotopically equivalent) can be seen in the development of the superior colliculus (Cooper and Rakic, '83). The nature of the cue that initiates this differential maturation, which events in cellular maturation it affects, and why it is separate from neurogenetic gradients are all areas for further study.

Late generation of displaced amacrine cells

"Displaced" amacrine cells, amacrine cells in the ganglion cell layer, constitute 40–50% of the ganglion cell layer's population in rodents (Perry, '81; Perry and Walker, '80a), and their origin has been a matter of question. In a study of the mouse retina, Hinds and Hinds ('83) failed to find sufficient numbers of axonless cells in the ganglion cell layer early in development to account for the size of the displaced amacrine cell population. To explain this disparity, they suggested that amacrine cells could arise from retinal ganglion cells that lose their axons. Our finding that cells of amacrine morphology are produced later in development, and undergo a prolonged migration, suggests that the failure to find axonless cells in the ganglion cell layer early in development is not due to their derivation from ganglion cells but simply to their late appearance, consistent with the observations of Perry et al. ('83). It is interesting that a synaptic target population of these cells (the retinal ganglion cells) is in place and has undergone a substantial amount of cell degeneration prior to interneuronal migration into the ganglion cell layer.

Creation of the central specialization of the hamster retina

Like every other mammalian retina examined to date (Stone, '83), the hamster has a streaklike elevation in gan-

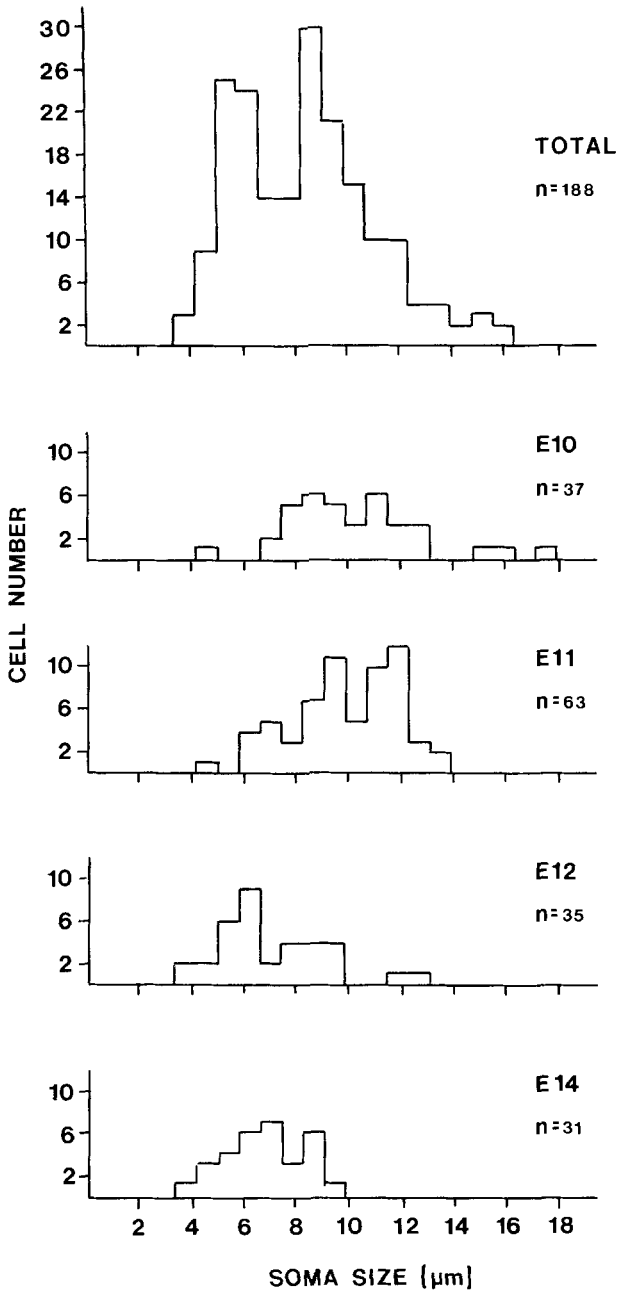

Fig. 12. Distribution of the number of cells by soma diameter (μm) in the ganglion cell layer at postnatal day 30. The overall size distribution is shown (top) as well as the distribution of cells labeled after ^{3}H thymidine injections at embryonic days 10, 11, 12, or 14.

glion cell density falling roughly along the horizontal meridian, a relatively small elevation compared to that seen in other species (Sengelaub et al., '83). Four mechanisms have been considered that could create this differential cell density, which are not necessarily mutually exclusive: (1) greater generation of cells centrally; (2) greater death of cells peripherally; (3) greater growth of the retina peripherally; and (4) migration of cells toward the central retina. These data suggest that in the hamster, the initial generation of cells is uniform, or perhaps slightly elevated in the periphery; that in some embryonic cohorts, more cells die in the retinal periphery during the period of maximal cell death; and after that, in the late postnatal period, a common factor which is most probably retinal growth reduces the density of all embryonic cohorts in the retinal periphery.

There is no evidence for greater generation of cells centrally than peripherally. Only on the first day of generation are cells produced in greater numbers centrally, and the difference (22% more centrally) is well below the adult difference (56% more centrally). On every other day of generation, cells continue to be generated centrally but more cells are produced in the peripheral retina. This result has uniform support across species: even in species (cat and human) with marked central specializations, more cells may be produced centrally, but the disparity in initial generation is well below the adult disparity (Henderson et al., '85; Stone et al., '82; Beazley and Dunlop, '83; Provis et al., '85).

Differential cell death appears to contribute to the creation of the central specialization of the retina in the hamster. Overall, more cells degenerate in the retinal periphery during the period of cell death (Fig. 3). Counts of ^{3}H thymidine-labeled degenerating cells show this differential degeneration to be confined principally to the E10 and E11 cohorts (Fig. 9), which at maturity are large cells of ganglion cell morphology. The absolute loss of cells from P4 to P6 is consistent with this finding as is the change in the relative distribution of cell densities from P6 to P10, showing relative density reductions in the periphery only in these cohorts (Fig. 10). Finally, the emergence of center to periphery differences in cell distribution in the ganglion cell layer (Fig. 2, P5–P10) and the appearance of differential degeneration are temporally congruent (Fig. 3).

The late postnatal development of the central specialization in the hamster appears to depend on a single factor that reduces relative peripheral cell density in all embryonic cohorts (Fig. 11), which is most likely to be retinal growth. Coincident differential death or migration in all cohorts cannot be ruled out, but we can present no independent evidence for these factors. It is interesting to consider whether the early differential death might directly cause the later differential growth. For example, if we imagine the spherical expansion of the retina to be like blowing up a balloon that is not of uniform thickness or strength, a small differential loss of cells in the periphery might predispose toward greater relative expansion there.

In the quokka, migration of cells from the peripheral to central retina has been suggested as a way in which the periphery might be depleted of cells while cells are added centrally, with no net change in cell number (Beazley and Dunlop, '83). This possibility seems unlikely on a number of counts for the development of the rodent retina. For example, postnatal changes in total cell number in the retinal ganglion cell layer do occur in both the hamster (this study) and the rat (Perry et al., '83). Although the central losses are not so great as those seen in the periphery, cell number is decreased centrally over the period in which the central specialization begins to develop; if cells were migrating centrally at this time, cell degeneration would have to be higher centrally than peripherally to counteract the influx of cells. In fact, the cell degeneration centrally is lower. Whether this difference is a real differ-

ence between species or a difference in interpretation remains to be determined.

Why greater risk of mortality in the first-generated cohorts and in the retinal periphery?

We suggest that the greater cell death in the first-generated cohorts is due directly to the greater death of peripherally located cells of these cohorts. These cohorts consist of a particular cell type (with x- or y-type decussation properties; Drager, '84) that at adulthood preferentially represent the central retina. We hypothesize that this preferential representation results from early losses of these cells in the retinal periphery. This hypothesis is obviously far from proven, and there are several other interesting candidate hypotheses: for example, the earliest-generated cells could serve as pioneers in the early establishment of projection laterality, with incorrectly projecting cells being removed by death.

The mechanisms of the greater death in the retinal periphery in certain cell groups are not clear. Greater probability of cell death by retinal location could be intrinsic, preprogrammed, and independent of competition for terminal sites. It could also be the result of differential success in acquiring afferents or targets. Spatial gradients in generation, maturation, and synaptogenesis have been reported for retinal targets (Crossland and Uchwat, '82; Cooper and Rakic, '83). It could be the case that early in development, the central target fields of the peripheral retina are immature compared to those for central retina, and that peripheral retinal cells fail to establish their connectivity due to simple unavailability. Alternatively, a differential distribution of an adhesivity factor in afferents (Fraser, '80) at a central target could account for the differential success of neurons in establishing their connections. Failure to establish connections could result in a restriction of early arbor and the eventual death of the cell.

In previous studies, we have observed spatial inhomogeneities in cell death in a variety of structures (Finlay et al., '82; Finlay and Slattery, '83; Janowsky and Finlay, '83; Sengelaub et al., '85). The superficial gray layer of the colliculus shows more cell degeneration in its retinotopic periphery, while the intermediate and deep gray layers show greater cell loss centrally. Almost all of the cell degeneration visible in the dorsal lateral geniculate body occurs in its retinotopic periphery, while the ventral lateral geniculate shows no spatial inhomogeneities. These differences correspond in a very interesting way to the known differences in the representation of the central and peripheral visual field in these structures. They suggest that one of the ways preferential representation of part of the visual field may be established is by the differential success of subpopulations of neurons in establishing their connections and surviving. Thus, a new function for the overproduction and death of neurons in the developing nervous system may be to create local specializations in larger neuronal arrays.

ACKNOWLEDGMENTS

We thank Candace Cornell, Lisa Kurz, Ken Wikler, and Martha Windrem for technical assistance, and Lisa Hudson for statistical consultation. This research was supported by NSF grant BNS 74 14941, NIH Career Development Award 1 K04 NS00783, and Research Award R01 NS19245 to B. Finlay, and a Grant-in-Aid of Research to D. Sengelaub.

LITERATURE CITED

Abercrombie, M. (1946) Estimation of nuclear populations from microtome sections. Anat. Rec. *94:*239–247.

Beazley, L.D., and S.A. Dunlop (1983) The evolution of an area centralis and visual streak in the ganglion cell layer of the marsupial *Setonix brachyuris*. J. Comp. Neurol. *216:*211–231.

Braekevelt, C.R., and M.J. Hollenberg (1970) The development of the retina of the albino rat. Am. J. Anat. *127:*281–302.

Carter-Dawson, L.D., and M.M. LaVail (1979) Rods and cones in the mouse retina, II. Autoradiographic analysis of cell generation using tritiated thymidine. J. Comp. Neurol. *188:*263–272.

Chalupa, L.M., and I. Thompson (1980) Retinal ganglion cell projections to the superior colliculus of the hamster demonstrated by the horseradish peroxidase technique. Neurosci. Lett. *19:*13–19.

Chu-Wang, I.-W., and R.W. Oppenheim (1978) Cell death of motoneurons in the chick embryo spinal cord. I. A light and electron microscopic study of naturally occurring and induced cell loss during development. J. Comp. Neurol. *177:*33–58.

Cooper, M.L., and P. Rakic (1983) Gradients of cellular maturation and synaptogenesis in the superior colliculus of the fetal rhesus monkey. J. Comp. Neurol. *215:*165–186.

Crossland, W.J., and C.J. Uchwat (1982) Neurogenesis in the central visual pathways of the golden hamster. Dev. Brain Res. *5:*99–103.

Cunningham, T.J., J.M. Mohler, and D.L. Giordano (1981) Naturally occurring death in the ganglion cell layer of the neonatal rat: Morphology and evidence for regional correspondence with neuron death in the superior colliculus. Dev. Brain Res. *2:*203–215.

Drager, U.C. (1984) Time of origin of ganglion cells giving rise to crossed and uncrossed projections in the mouse retina. Soc. Neurosci. Abstr. *10:*141.

Finlay, B.L., and M. Slattery (1983) Local differences in the amount of early cell death in neocortex predict adult local specializations. Science *219:*1349–1351.

Finlay, B.L., A.T. Berg, and D.R. Sengelaub (1982) Cell death in the mammalian visual system during normal development: II. Superior colliculus. J. Comp. Neurol. *204:*318–325.

Fraser, S.E. (1980) A differential adhesion approach to the patterning of nerve connections. Dev. Biol. *79:*453–464.

Frost, D.O., K.-F. So, and G.E. Schneider (1979) Postnatal development of retinal projections in Syrian hamsters: A study using autoradiographic and anterograde degeneration techniques. Neuroscience *4:*1649–1677.

Henderson, Z., K.C. Wikler, and B.L. Finlay (1985) Developmental changes in cell death and retinal ganglion cell distribution in the postnatal ferret retina. Soc. Neurosci. Abstr. *11:*15.

Hinds, J.W., and P.L. Hinds (1983) Development of retinal amacrine cells in mouse embryo: Evidence for two modes of formation. J. Comp. Neurol. *213:*1–23.

Janowsky, J.S., and B.L. Finlay (1983) Cell degeneration in early development of the forebrain and cerebellum. Anat. Embryol. *167:*439–447.

Jhaveri, S., and G.E. Schneider (1983) Relationship of lateral geniculate neuron migration to stages of optic tract growth in the hamster. Soc. Neurosci. Abstr. *9:*702.

Mastronarde, D.N., M.A. Thibeault, and M.W. Dubin (1984) Non-uniform postnatal growth of the cat retina. J. Comp. Neurol. *228:*598–608.

Morest, D.K. (1970) The pattern of neurogenesis in the retina of the rat. Z. Anat. Entwicklungsgesch. *131:*45–67.

Perry, V.H. (1981) Evidence for an amacrine cell system in the ganglion cell layer of the rat retina. Neuroscience *6:*931–944.

Perry, V.H., and M. Walker (1980a) Amacrine cells, displaced amacrine cells, and interplexiform cells in the retina of the rat. Proc. R. Soc. Lond. [Biol.] *208:*415–431.

Perry, V.H., and M. Walker (1980b) Morphology of cells in the ganglion cell layer during development of the rat retina. Proc. R. Soc. Lond. [Biol.] *208:*433–445.

Perry, V.H., Z. Henderson, and R. Linden (1983) Postnatal changes in retinal ganglion cell and optic axon populations in the pigmented rat. J. Comp. Neurol. *219:*356–368.

Potts, R.A., B. Dreher, and M.R. Bennet (1982) The loss of ganglion cells in the developing retina of the rat. Dev. Brain Res. *3:*481–486.

Provis, J.P., D. van Driel, F.A. Billson, and P. Russell (1985) Development of the human retina: patterns of cell distribution and redistribution in the ganglion cell layer. J. Comp. Neurol. *233*:429–451.

Raabe, J.I., M.S. Windrem, and B.L. Finlay (1985) Control of cell number in the developing visual system: III. Effects of visual cortex ablation. Dev. Brain Res. (in press).

Rager, G., and U. Rager (1978) Systems matching by degeneration. I.A quantitative electron microscopic study of the generation and degeneration of retinal ganglion cells in the chicken. Exp. Brain Res. *33*:65–78.

Rakic, P., and K.P. Riley (1983) Overproduction and elimination of retinal axons in the fetal rhesus monkey. Science *219*:1441–1444.

Rapaport, D.H., and J. Stone (1982) The site of commencement of maturation in the mammalian retina: observations in cat. Dev. Brain Res. *5*:273–279.

Sengelaub, D.R., and B.L. Finlay (1981) Early removal of one eye reduces normally occurring cell death in the remaining eye. Science *213*:573–574.

Sengelaub, D.R., and B.L. Finlay (1982) Cell death in the mammalian visual system during normal development: I. Retinal ganglion cells. J. Comp. Neurol. *204*:311–317.

Sengelaub, D.R., L.F. Jacobs, and B.L. Finlay (1985) Regional differences in normally occurring cell death in the hamster lateral geniculate nuclei. Neurosci. Lett. *55*:103–108.

Sengelaub, D.R., M.S. Windrem, and B.L. Finlay (1983) Alterations in adult retinal ganglion cell distribution following early monocular enucleation. Exp. Brain Res. *52*:269–276.

Sidman, R.L. (1961) Histogenesis of the mouse retina studied with thymidine 3-H. In G.K. Smelser (ed): The Structure of the Eye. New York: Academic Press, pp. 487–506.

Sidman, R.L. (1970) Autoradiographic methods and principles for study of the nervous system with thymidine 3-H. In W.J.H. Nauta and S.O.E. Ebbesson (eds): Contemporary Research Methods in Neuroanatomy. New York: Springer-Verlag, pp. 252–274.

Silver, J., and A.F.W. Hughes (1973) The role of cell death during morphogenesis of the mammalian eye. J. Morphol. *140*:159–170.

Stone, J. (1983) Parallel Processing in the Visual System. The Classification of Retinal Ganglion Cells and its Impact on the Neurobiology of Vision. New York: Plenum, pp. 265–325.

Stone, J., D.H. Rapaport, R.W. Williams, and L.M. Chalupa (1982) Uniformity of cell distribution in the ganglion cell layer of the prenatal cat: Implications for mechanisms of retinal development. Dev. Brain Res. *2*:231–242.

Walsh, C., E.H. Polley, T.L. Hickey, and R.W. Guillery (1983) Generation of cat's retinal ganglion cells in relation to central pathways. Nature *302*:611–614.

Wikler, K.C., J.I. Raabe, and B.L. Finlay (1985) Temporal retina is preferentially represented in the early retinotectal projection in the hamster. Dev. Brain Res. *21*:152–155.

Wikler, K.C., J. Kirn, M.S. Windrem, and B.L. Finlay (1985) Control of cell number in the developing visual system: II. Effects of partial tectal ablation. Dev. Brain Res. (in press).

Williams, R.W., M.J. Bastiani, and L.M. Chalupa (1983) Loss of axons in the cat optic nerve following fetal unilateral enucleation: An electron microscopic analysis. J. Neurosci. *3*:133–144.

Young, R.W. (1984) Cell death during differentiation of the retina in the mouse. J. Comp. Neurol. *229*:362–373.